RSC Advances

PAPER

View Article Online
View Journal | View Issue

Cite this: *RSC Adv.*, 2017, **7**, 46832

A novel dual-channel chemosensor for CN^- based on rhodamine B hydrazide derivatives and its application in bitter almond†

Peng-Xiang Pei, Jing-Han Hu,* Peng-Wei Ni, Chen Long, Jun-Xia Su and You Sun

In this article, we successfully designed and synthesized a novel chemosensor **PW** bearing rhodamine B hydrazide and 8-formyl-7-hydroxyl-4-methylcoumarin, which displayed both colorimetric and "turn-on" fluorescence responses for CN^- in DMSO/H_2O (1 : 1, v/v, pH = 7.20) solution. The probe could distinguish CN^- *via* a deprotonation process and the mechanism of intramolecular charge transfer (ICT), which was proved by ^1H NMR titration, ESI-MS and DFT calculations. The detection limit of the sensor **PW** towards CN^- was 1.592×10^{-7} M. Moreover, the sensor **PW** was successfully utilized to detect CN^- in bitter almond. Test strips containing **PW** were also prepared, which could act as a colorimetric tool to detect CN^- in practical application.

Received 19th August 2017
Accepted 27th September 2017

DOI: 10.1039/c7ra09174e

rsc.li/rsc-advances

1. Introduction

In recent years, the design and exploration of artificial sensors for recognizing cations and anions have received immense interest due to their important roles in biological, environmental, and industrial processes.[1–4] It is well known that CN^- is considered as the most hazardous one of various anions, and it is lethal to humans at concentrations of 0.5–3.5 mg kg^{-1} body weight.[5–7] However, trace amounts of CN^- also affect many functions such as blood vessels, visual sense, central nervous, heart and metabolic systems[8–11] in the human body. The World Health Organization (WHO) has set the maximum acceptable amount of 1.9 μM for cyanide ion in drinking water.[12,13] However, cyanide salts are widely utilized in various industries such as gold extraction, synthetic fibers, electroplating, and metallurgy *etc.*,[14–16] which lead to a serious harm to environment and human health. Thus, the rational design and synthesis of efficient sensors to selectively recognize CN^- is significantly important.

In the past few decades, a variety of analytical methods such as ion chromatography, potentiometric, titrimetric and electrochemical methods[17–20] have been reported for the investigation of CN^-. However, those methods usually suffer from a series of shortages like high cost, long response time, sophisticated equipment and so on, which are serious stumbling blocks to its practical application.[21–23] In contrast, fluorometric and colorimetric sensors have gained more attention due to low cost, simplicity, high selectivity, sensitivity and fast response.[24]

Our research group has a longstanding interest in molecular recognition.[25–39] Herein, we designed a novel chemosensor **PW** based on rhodamine B hydrazide derivatives, which showed a dual-channel response for CN^- in DMSO/H_2O (1 : 1, v/v, pH = 7.20) solution. To the best of our knowledge,[29–33] most of sensors based on rhodamine B derivatives were mainly utilized on the recognition of metal ions, and were rarely reported for the recognition of anions, especially for CN^-. Furthermore, we found that sensors based on rhodamine B derivatives usually recognized metal ions by opening rings, however, the sensor **PW** recognized CN^- by deprotonation process, and the ring had no any change in **PW**. In addition, the reason for the introduction of rhodamine B is owe to its good water solubility and strong fluorescence, which makes clearer for recognition of CN^- in real sample. On account for these advantages, we believe that the sensor **PW** shows great promise for its potential applications.

2. Experimental

2.1. Reagents and apparatus

All reagents and solvents were obtained from the commercial sources without further purification. Double-distilled water was used throughout the experiment. Tetrabutylammonium salt of anions (F^-, Cl^-, Br^-, I^-, AcO^-, $H_2PO_4^-$, ClO_4^- and HSO_4^-) and sodium salt of anions (CN^- and SCN^-) were purchased from Alfa-Aesar Chemical Reagent Co. and stored in vacuum desiccators. ^1H NMR and ^{13}C NMR spectra were respectively recorded on a Mercury-400BB spectrometer at 400 MHz and 100 MHz, and chemical shifts were recorded in ppm (DMSO-d_6 as solvent). Melting points were measured on an X-4 digital

College of Chemical and Biological Engineering, Lanzhou Jiaotong University, Lanzhou, gansu, 730070, P. R. China. E-mail: hujinghan62@163.com

† Electronic supplementary information (ESI) available. CCDC 1563205. For ESI and crystallographic data in CIF or other electronic format see DOI: 10.1039/c7ra09174e

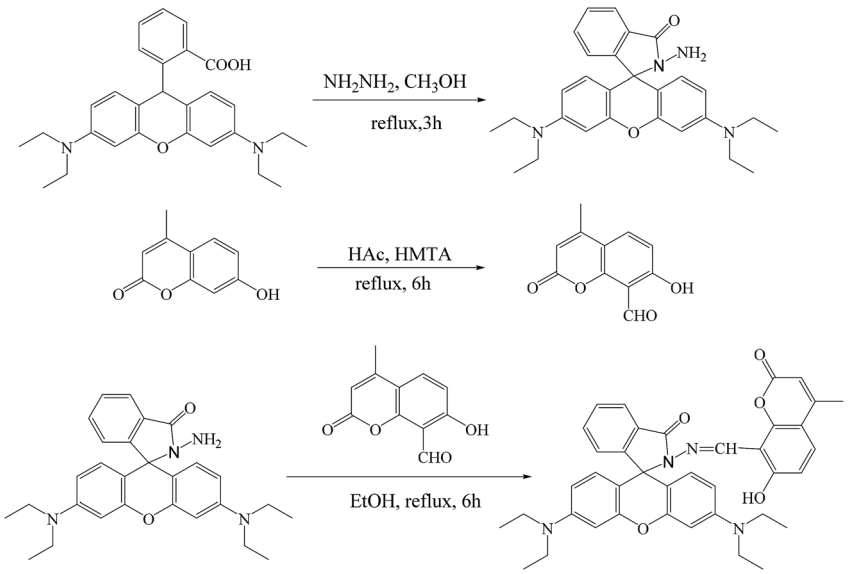

Scheme 1 The synthesis process of **PW**.

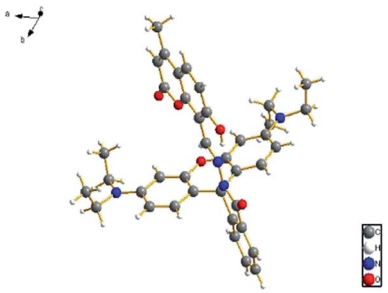

Fig. 1 Single-crystal X-ray structure of sensor **PW**.

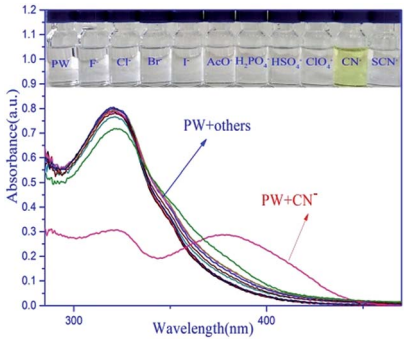

Fig. 2 UV-Vis spectra of **PW** (20 μM) in the presence of 50 equiv. of various anions in DMSO/H_2O (1 : 1, v/v, pH = 7.20) binary solution at room temperature. Inset: color changes of **PW** containing various anions in DMSO/H_2O (1 : 1, v/v, pH = 7.20) solution.

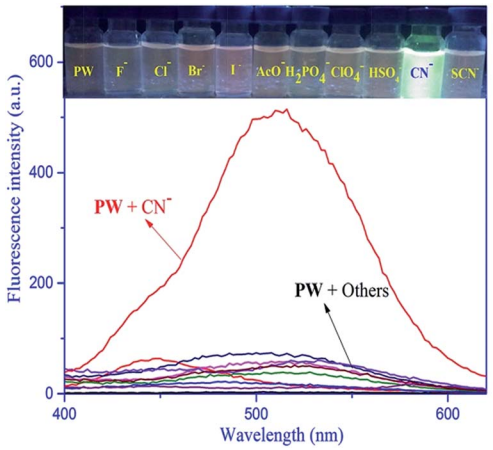

Fig. 3 Fluorescence spectra of **PW** (20 μM, λ_{ex} = 320 nm, λ_{em} = 512 nm) with various anions (50 equiv.) in DMSO/H_2O (1 : 1, v/v, pH = 7.20). Inset: color changes observed for **PW** (20 μM) with various anions (50 equiv.) in DMSO/H_2O (1 : 1, v/v, pH = 7.20) solution under the UV lamp.

melting point apparatus that was uncorrected. Fluorescence spectra were performed using a Shimadzu RF-5301 fluorescence spectrophotometer. UV-Vis absorption spectra were measured on a Shimadzu UV-2550 spectrometer. ESI-MS was measured on an Agilent 1100 LC-MSD-Trap-VL system.

2.2. Synthesis of 8-formyl-7-hydroxyl-4-methylcoumarin

4-Methylumbelliferone (10 g, 0.057 mol) and methenamine (20 g, 0.143 mol) were mixed in acetic acid (75 ml), and refluxed for 5.5 h at 95 °C, then added 150 ml hydrochloric acid (HCl/H_2O, v/v = 84 : 100) and continued to stir for 0.5 h. Cooling to room temperature, poured the reaction solution to 750 ml distilled water and used acetic ether (300 ml) to extract, afterwards, the acetic ether was washed two times with saturated salt water, and the extract was evaporated to dry, finally, the extractive was recrystallized with EtOH to obtain yellow granular compound in 13%, mp: 179–181 °C.

2.3. Synthesis of intermediate rhodamine B hydrazide

Intermediate rhodamine B hydrazide was prepared by one step condensation reflux reaction of rhodamine B (0.96 g, 2 mmol)

and hydrazine hydrate (1 ml, 0.02 mol) in methanol (30 ml), the reaction was stirred for 3 h at 65 °C, after cooling to room temperature, adjusting pH to 8–9, which emerged lots of pale pink precipitate, then filtrated and washed three times with distilled water to obtain light pink compound in 81% yield, mp: 215–217 °C.

2.4. Synthesis of PW

Rhodamine B hydrazide (0.46 g, 1 mmol) and 8-formyl-7-hydroxyl-4-methylcoumarin (0.25 g, 1.2 mol) were refluxed for 6 h in DMF (20 ml) at 85 °C, after cooling to room temperature, the precipitate was filtrated and recrystallized with DMF-H_2O to get light brown compound in 62% yield. As shown in Scheme 1 mp > 300 °C. ^{1}H NMR (DMSO-d_6, 400 MHz, ppm) δ: 11.74 (s, 1H), 9.49 (s, 1H), 7.97 (d, J = 8.38 Hz, 2H), 7.66 (dd, J = 7.60 Hz, 2H), 7.53 (d, J = 8.38 Hz, 1H), 7.17 (d, J = 7.40 Hz, 1H), 6.75 (d, J = 8.87 Hz, 1H), 6.46 (d, J = 8.76 Hz, 3H), 6.37 (m, 2H), 6.16 (s, 1H), 3.30 (d, J = 7.70 Hz, 8H) 2.29 (s, 3H), 1.07 (d, J = 6.86 Hz, 12H). ^{13}C NMR (DMSO-d_6, 100 MHz, ppm) δ: 164.05, 162.69, 161.06, 159.03, 153.67, 152.77, 151.38, 153.25, 149.12, 145.18, 134.83, 129.52, 128.73, 128.61, 128.25, 124.47, 123.66, 113.68, 112.08, 111.20, 108.76, 105.80, 104.42, 103.57, 97.81, 66.12, 44.10, 36.19, 31.19, 18.58, 12.76. m/z (ES^+) calcd for $C_{39}H_{38}N_4O_6$: $[M + H^+]$ = 642, found: 643.2830. The structure of sensor **PW** was further confirmed by single-crystal X-ray diffraction (Fig. 1).

3. Results and discussion

The anion-sensing abilities of **PW** were investigated by UV-Vis spectroscopy and fluorescence spectroscopy in DMSO/H_2O

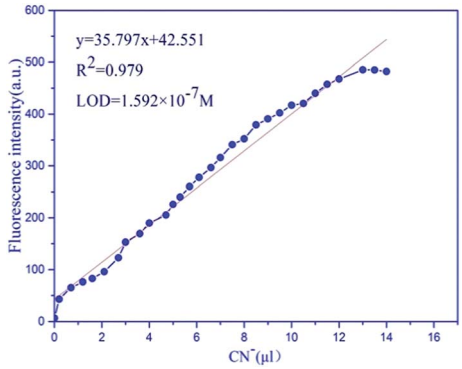

Fig. 6 Fluorescence detection limit of **PW** (20 μM) towards CN^- in DMSO/H_2O (1 : 1, v/v, pH = 7.20) solution.

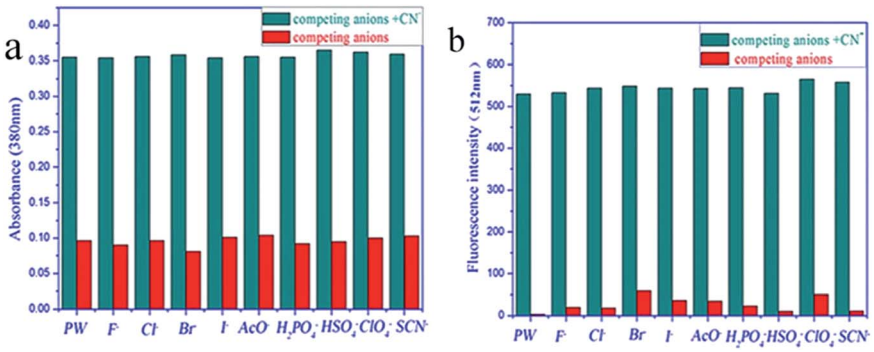

Fig. 4 (a) UV-Vis spectra changes for **PW** (20 μM) containing various anions in presence of CN^- in DMSO/H_2O (1 : 1, v/v, pH = 7.20) solution. (b) Fluorescence spectra of **PW**–CN^- with various interference anions in DMSO/H_2O (1 : 1, v/v, pH = 7.20) solution.

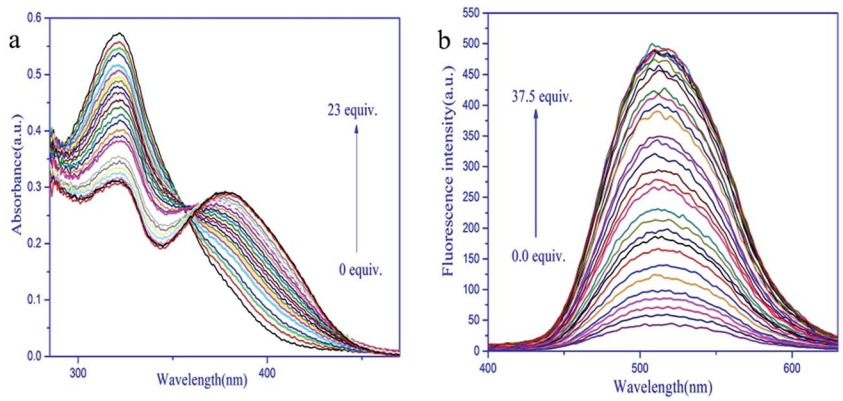

Fig. 5 (a) Absorption spectra titration of sensor **PW** (20 μM) after addition of different concentration of CN^- (0–23 equiv.) in DMSO/H_2O (1 : 1, v/v, pH = 7.20) solution (b) fluorescence spectra of **PW** in the presence of different concentration of CN^- (0–37.5 equiv.) in DMSO/H_2O (1 : 1, v/v, pH = 7.20) solution.

(1 : 1, v/v, pH = 7.20). When 50 equiv. various anions (F^-, Cl^-, Br^-, I^-, AcO^-, $H_2PO_4^-$, HSO_4^-, ClO_4^-, SCN^- and CN^-) were respectively added to the solution of **PW** (2.0×10^{-5} M), only CN^- was found to induce a dramatic color change from colorless to yellow. In the corresponding UV-Vis spectra, a dramatic absorption band was appeared. However, other examined anions (F^-, Cl^-, Br^-, I^-, AcO^-, $H_2PO_4^-$, HSO_4^-, ClO_4^- and SCN^-) didn't induce any dramatic changes in color and absorption spectra (Fig. 2). These results suggested that **PW** could recognize CN^- over all other anions.

Free **PW** alone exhibited a weak fluorescence emission band at 512 nm when excited at 320 nm in DMSO/H_2O (1 : 1, v/v, pH = 7.20), up addition of 50 equiv. CN^- to the solution of **PW** (2.0×10^{-5} M), **PW** induced a significant fluorescence 'off-on' response for CN^- at 512 nm, as shown in Fig. 3, which responded with a color change from saffron yellow to bright green under UV lamp. However, other anions (F^-, Cl^-, Br^-, I^-, AcO^-, $H_2PO_4^-$, HSO_4^-, ClO_4^- and SCN^-) hardly changed the color and fluorescence intensity of **PW**, which indicated that **PW** could sense CN^- with single selectivity in DMSO/H_2O (1 : 1, v/v, pH = 7.20) solution.

To validate anti-interference capability of sensor **PW**, **PW** containing various anions (F^-, Cl^-, Br^-, I^-, AcO^-, $H_2PO_4^-$, HSO_4^-, ClO_4^- and SCN^-) were investigated by UV-Vis spectroscopy and fluorescence spectroscopy. Results suggested that **PW** solutions with various anions didn't induce distinct spectrum changes in absence of CN^-, however, upon addition of CN^-, as shown in Fig. 4, all solutions showed obviously spectrum changes, which indicated that sensor **PW** had an excellent selectivity for CN^- over other anions no matter in UV-Vis spectroscopy and fluorescence spectroscopy.

Furthermore, we calculated the quantum yields of **PW** and **PW** + CN^- by measuring respectively the UV-Vis absorption spectra and the fluorescent spectra and the reference compound. The quantum yields were calculated using the following equation:[40]

$$\varphi_1 = \varphi_2 \times \frac{F_1}{F_2} \times \frac{A_2}{A_1}$$

(where φ_1 is the quantum yield of **PW** and **PW** + CN^-. φ_2 is the quantum yield of reference compound (quinine sulfate, φ_2 = 0.55). F_1 is the fluorescent integral of **PW** and **PW** + CN^-. F_2 is the fluorescent integral of reference compound. A_1 is the absorbance of **PW** and **PW** + CN^-. A_2 is the absorbance of reference compound). The quantum yield of **PW** and **PW** + CN^- were 0.0434 M and 0.8916 respectively.

To get insight into the CN^- (0.01 M) sensing property of sensor **PW**, the UV-Vis absorption spectrum and fluorescence spectrum changes of **PW** were carried out in DMSO/H_2O (1 : 1, v/v, pH = 7.20) solution. As shown in Fig. 5a, along with the increasing amount of CN^- from 0 equiv. to 23 equiv., the absorption band at 320 nm decreased while the absorption band at 380 nm increased. At the same time, the well-defined isosbestic point appeared at 358 nm, which clearly indicated an interconversion into single discrete chemical species during the titration process. Fig. 5b showed the emission spectrum changes on addition of CN^-, when excited at 320 nm, the emission intensity at 512 nm of sensor **PW** enhanced 11-fold on changing the concentration of CN^- from 0 equiv. to 37.5 equiv. Furthermore, the fluorescence detection limits of **PW** towards CN^- based on $3S_B/S$ (where S_B is the standard deviation of the blank solution and S is the slope of the calibration curve) was

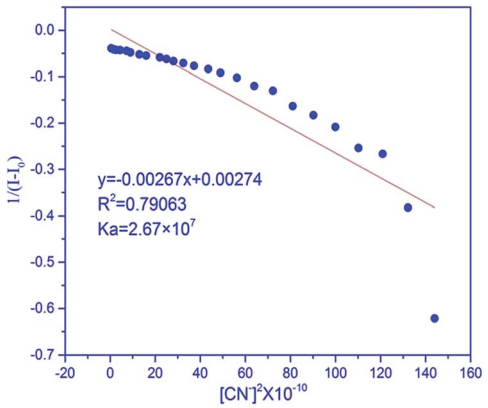

Fig. 7 Benesi–Hilderbrand plot of **PW** with CN^-.

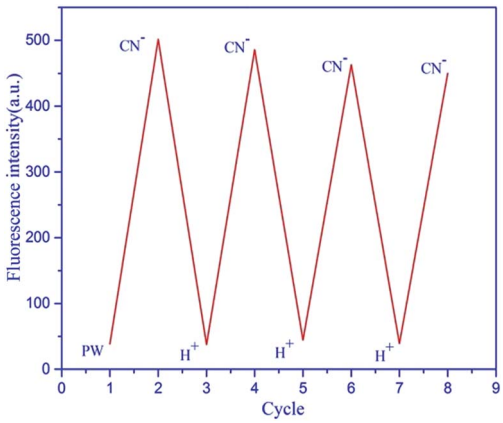

Fig. 8 The reversible and reproducible fluorometric switch controlled by alternating addition of H^+ and CN^-.

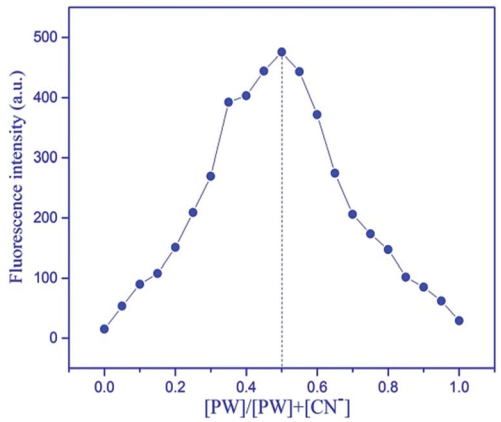

Fig. 9 Job plots of **PW** and CN^-.

down to 1.592×10^{-7} M (Fig. 6), which indicated that **PW** could detect low concentration of CN^- in practical application.

The association constants (K_a) were determined based on the fluorescent titration curve using the equation as follows: where F_1 and F_0 respectively represent the fluorescent intensity of host in the presence and absence of ions, F_{max} is the saturated intensity of host in the presence of excess amounts of ions; [C] is the concentration of ions added.[41]

$$1/(F_{max} - F_0) = 1/(F_1 - F_0)(1/(K[C]^2) + 1)$$

According for formula above, as shown in Fig. 7, the acid reaction equilibrium constant (K_a) is 2.67×10^7, and $pK_a = 6.52$.

Since pH may affect the charge distribution of **PW** and change its inherent fluorescence properties, the impact of pH on **PW** was studied by fluorescence spectroscopy. As shown in Fig. S1,† sensor **PW** showed a significant fluorescence response for CN^- within the basic pH range from 7.0 and 9.0, indicating clearly that pH had a significant influence on the recognition of CN^-.

The reversibility of sensor **PW** was measured by alternating addition of H^+ and CN^- in DMSO/H_2O (1 : 1, v/v, pH = 7.20) solution. As shown in Fig. 8, upon addition of H^+ to the **PW**–CN^- system, the fluorescence intensity clearly showed "OFF" behavior through the regeneration of **PW**. On further addition of CN^-, the fluorescence intensity showed "ON" through the deprotonation of **PW**. This indicated that sensor **PW** showed an excellent reversibility for CN^- ions, and the "OFF-ON-OFF" switching process could be repeated more than seven times without larger fluorescence loss.

To confirm the binding stoichiometry between **PW** and CN^-, the method of continuous variations was used as shown in Fig. 9. A job plot was implemented, as we expected, the results demonstrated that a stoichiometry for **PW**–CN^- was 1 : 1.

The recognition mechanism of sensor **PW** towards CN^- based on the deprotonation of hydroxyl was finally investigated by ^{1}H NMR titration and mass spectrometry. As shown in Fig. 10, sensor **PW** showed two strong peaks at 11.74 ppm and 9.49 ppm in DMSO-d_6, which correspond to the proton of –OH and N=CH, upon the addition of 2.5 equiv. CN^-, the –OH peak at 11.74 ppm disappeared, which indicated that CN^- took the protons of –OH due to strong acid was readily deprotonated when basic ions existed, furthermore, we found that the peak of N=CH gradually decreased and showed upfield shift, which indicated that the deprotonation of hydroxyl made sensor **PW** shielded by the increase of electron density through charge delocalization in the conjugated system. Afterwards, addition of 3.0 equiv. H^+ to the above system, we found that there appeared two new peaks at 11.74 ppm and 9.49 ppm, which can be attributed to the –NH and –OH.

ESI-MS also gave a strong support for the mechanism of **PW** towards CN^-, as shown in Fig. S3,† **PW** ion peak was detected at m/z 643.2830 (**PW** + H^+), but it appeared at m/z 665.3495 (**PW**–H^+ + Na^+ + H^+) after the addition of CN^- (Fig. S4†), which indicated that **PW** did undergo deprotonation process.

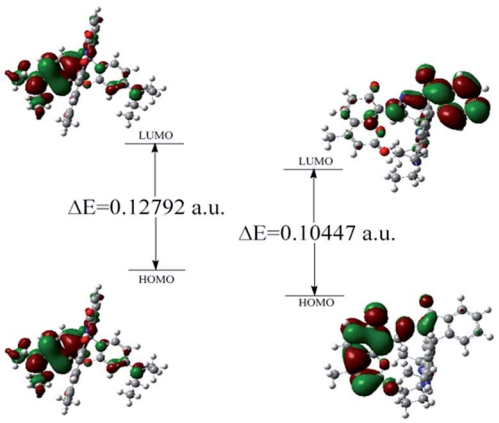

Fig. 11 The DFT computed HOMO and LUMO diagram of **PW** and **PW**–CN^- system.

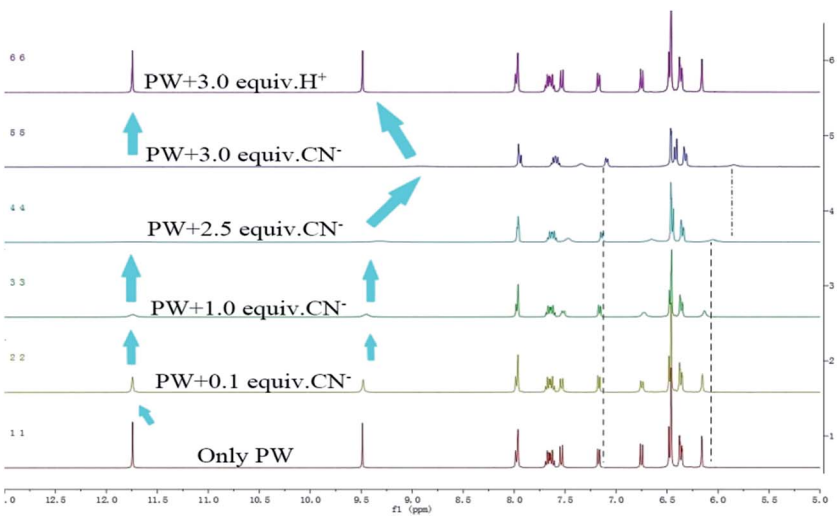

Fig. 10 ^{1}H NMR spectra of free **PW** (DMSO-d_6) and in the presence of different amounts of CN^- (0.1 M, DMSO-d_6).

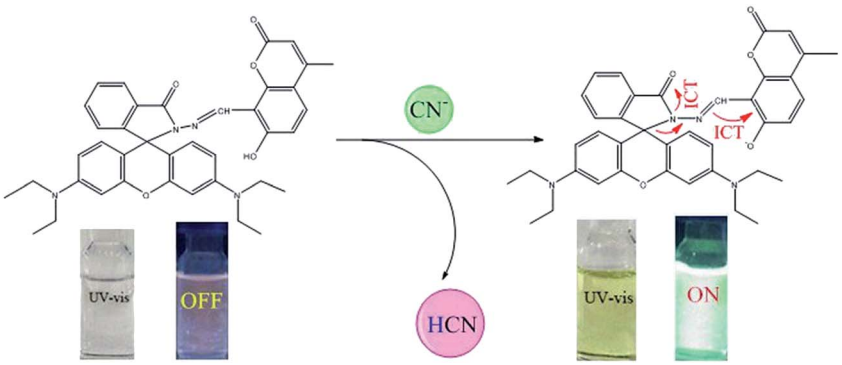

Scheme 2 A possible mechanism of **PW** and CN^-.

Further analysis of the mechanism of **PW** with CN^-, we performed DFT calculations done at the B3LYP/6-311g (2d, p) level of theory.[34] As shown in Fig. 11, the HOMO–LUMO energy band gap of **PW** and **PW**–CN^- system were respectively 0.12792 a.u. and 0.10447 a.u. Obviously, the HOMO–LUMO energy band gap of **PW** was higher than the **PW**–CN^- system, which showed the reaction could occur in dynamics. Furthermore, we could observe that the electron cloud density of the HOMO levels of **PW** are almost localized on the ring of rhodamine B, upon interaction with CN^-, the electron cloud of the HOMO levels of **PW** shifted the ring of coumarin, which clearly indicated that the addition of CN^- made sensor **PW** occur intramolecular charge transfer (ICT).

This deprotonation caused an obvious change in absorption spectra, and the fluorescence enhancement at 512 nm was possibly caused by a large charge separation resulting in a strong intramolecular charge transfer (ICT) in **PW**, simultaneously, we also confirmed that the stoichiometry of **PW**–CN^- was 1 : 1. Based on the above findings, we proposed that a possible interaction mechanism between **PW** and CN^- in this system which may proceed through the route depicted in Scheme 2.

To facilitate the use of **PW** for the detection of cyanide in practical application, test strips were prepared by immersing filter papers into the DMSO solution of **PW** (0.01 M) and then drying in air. As shown in Fig. 12, interestingly, the color of test strip changed from bisque to dark yellow under visible light, and changed from ecru to green under UV lamp. This clearly indicated that test strips containing **PW** could act as a practical colorimetric tool to detect CN^-.

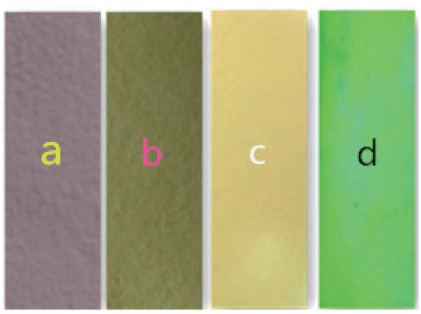

Fig. 12 Photographs of test strips (a) only **PW**; (b) **PW** with CN^- by naked eyes; (c) only **PW** under UV lamp; (d) **PW** with CN^- under UV lamp.

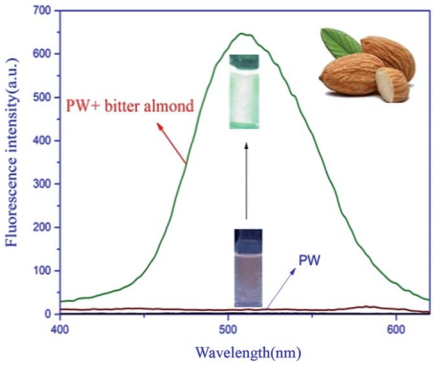

Fig. 13 Fluorescence spectra response of **PW** (20 μM) in diluted bitter almond.

To further investigate the practical application of sensor **PW** in our lives, we utilized it to detect CN^- in the bitter almond. 25 g of crushed bitter almond were put into a round flask containing 100 ml of water and 0.5 g of NaOH, the mixture solution was stirred for 20 min before filtrating. Then the filtrate was adjusted to pH = 9 with fresh double water, and the solution (2.0 ml) was added to the solution of **PW** (0.5 ml, 1.0×10^{-5} M), we found that the fluorescence intensity of **PW** remarkably enhanced, which clearly indicated that **PW** could be applied successfully for detecting CN^- in bitter almond (Fig. 13).

To further show excellent properties of **PW**, we also compared detection limits, solvent medium, and applications of reported sensors with compound **PW**, as shown in Table S1.†

4. Conclusion

In summary, we have designed and synthesized a novel chemosensor **PW**, which showed a dual-channel response for CN^- in DMSO/H_2O (1 : 1, v/v) solution within the basic pH range (pH = 7.0–9.0). The fluorescence process could be reversed by adding H^+ and CN^-, and the switching process could be repeated more

than seven times without a large fluorescence loss. Moreover, the detection limit on fluorescence response of the sensor **PW** to CN^- was down to 1.592×10^{-7} M by titration method, which is lower than the maximum level of 1.9×10^{-6} M for cyanide in drinking water according to WHO guidelines. Notably, the simple and efficient sensor **PW** was successfully used to the qualitative detection of cyanide in bitter almond. Test trips based on sensor **PW** were fabricated and could serve as a practical colorimetric tool to detect CN^- in field measurements. On account of those advantages, we believe that **PW** as a CN^- sensor makes it more conspicuous for its potential application.

Conflicts of interest

There are no conflicts to declare.

Acknowledgements

We gratefully acknowledge the support of the National Nature Science Foundation of China (No. 21467012).

References

1 W. J. Qu, T. B. Wei, Q. Lin, W. T. Li, J. X. Su, G. Y. Liang and Y. M. Zhang, *Sens. Actuators, B*, 2016, **232**, 115–124.
2 A. B. Davis, R. E. Lambert, F. R. Fronczek, P. J. Craggc and K. J. Wallace, *New J. Chem.*, 2014, **38**, 4678–4683.
3 G. C. Yu, Z. B. Zhang, C. Y. Han, M. Xue, Q. Z. Zhou and F. H. Huang, *Chem. Commun.*, 2012, **48**, 2958–2960.
4 C. Y. Han, F. Y. Ma, Z. B. Zhang, B. Y. Xia, Y. H. Yu and F. H. Huang, *Org. Lett.*, 2010, **12**, 4360–4363.
5 L. T. Zeng, N. Fan, J. Y. Zha, X. C. Hu, B. Q. Fu, C. Q. Qin and L. Wang, *Analyst*, 2013, **138**, 7083–7088.
6 S. K. Patra, S. K. Sheet, B. Sen, K. Aguan, D. R. Roy and S. Khatua, *J. Org. Chem.*, DOI: 10.1021/acs.joc.7b01743.
7 M. K. S. Flores, I. J. B. Rodríguez, D. M. Otero, M. A. G. Eleno, J. J. G. García, D. M. Morales and A. D. González, *Dalton Trans.*, 2017, **46**, 4950–4959.
8 J. Afshani, A. Badiei, M. Jafari, A. Shayesteh, M. Karimi, N. Lashgari and G. M. Ziarani, *J. Lumin.*, 2016, **179**, 463–468.
9 P. Gholamzadeh, G. M. Ziarani, N. Lashgari, A. Badiei, A. Shayesteh and M. Jafari, *J. Fluoresc.*, 2016, **26**, 1857–1864.
10 S. Goswami, A. Manna, S. Paul, K. Aich, A. K. Das and S. Chakraborty, *Tetrahedron Lett.*, 2013, **54**, 1785–1789.
11 A. Sarkar, S. Bhattacharyya and A. Mukherjee, *Dalton Trans.*, 2016, **45**, 1166–1175.
12 P. Zhang, B. B. Shi, X. M. You, Y. M. Zhang, Q. Lin, H. Yao and T. B. Wei, *Tetrahedron*, 2014, **70**, 1889–1894.
13 S. Das, S. Biswas, S. Mukherjee, J. Bandyopadhyay, S. Samanta, I. Bhowmick, D. K. Hazra, A. Ray and P. P. Parui, *RSC Adv.*, 2014, **4**, 9656–9659.
14 D. S. Kim, Y. M. Chung, M. Jun and K. H. Ahn, *J. Org. Chem.*, 2009, **74**, 4849–4854.
15 R. Manivannan, A. Satheshkumar and K. P. Elango, *New J. Chem.*, 2013, **37**, 3152–3160.
16 P. Li, H. Wang, M. Zhang, G. X. Zhang and D. Q. Zhu, *Org. Lett.*, 2009, **11**, 1943–1946.
17 C. Chen, R. Y. Wang, L. Q. Guo and N. Y. Fu, *Org. Lett.*, 2011, **13**, 1162–1172.
18 G. Y. Gao, W. J. Qu, B. B. Shi, P. Zhang, Q. Lin, H. Yao, W. L. Yang, Y. M. Zhang and T. B. Wei, *Spectrochim. Acta, Part A*, 2014, **121**, 514–613.
19 D. Shan, C. Mousty and S. Cosnier, *Anal. Chem.*, 2004, **6**, 178–182.
20 G. Y. Gao, B. Gong, W. T. Zhang, Q. L. Ye, J. Wei and G. L. Ning, *Spectrochim. Acta, Part B*, 2012, **162**, 391–412.
21 T. K. Ghorpade, M. Patri and S. P. Mishra, *Spectrochim. Acta, Part B*, 2016, **225**, 428–435.
22 S. Chattaraj and A. K. Das, *Analyst*, 1991, **116**, 739–741.
23 S. Yen, C. T. Wang and J. S. Wang, *Chem. Eng. Commun.*, 1991, **109**, 167–180.
24 W. K. Dong, X. L. Li, L. Wang, Y. Zhang and Y. J. Ding, *Spectrochim. Acta, Part B*, 2016, **229**, 370–378.
25 J. Qi, J. H. Hu, J. J. Chen, Y. Sun and J. B. Li, *Curr. Anal. Chem.*, 2016, **12**, 119–123.
26 J. H. Hu, Y. Sun, J. Qi, P. X. Pei, Q. Lin and Y. M. Zhang, *RSC Adv.*, 2016, **6**, 100401–100406.
27 J. H. Hu, Y. Sun, J. Qi, Q. Lin and T. B. Wei, *Spectrochim. Acta, Part A*, 2017, **175**, 125–133.
28 Y. Sun, J. H. Hu, J. B. Li and J. Qi, *Spectrochim. Acta, Part A*, 2016, **167**, 101–105.
29 J. H. Hu, J. B. Li, J. Qi and Y. Sun, *Spectrochim. Acta, Part B*, 2015, **208**, 581–587.
30 J. H. Hu, J. B. Li, J. Qi and Y. Sun, *New J. Chem.*, 2015, **39**, 4041–4046.
31 J. H. Hu, J. B. Li, J. Qi and Y. Sun, *Phosphorus, Sulfur Silicon Relat. Elem.*, 2016, **191**, 984–987.
32 J. H. Hu, J. B. Li, J. Qi and J. J. Chen, *New J. Chem.*, 2015, **39**, 843–848.
33 J. B. Li, J. H. Hu, J. J. Chen and J. Qi, *Spectrochim. Acta, Part A*, 2014, **133**, 773–777.
34 S. Z. Pu, H. C. Ding, G. Liu, C. H. Zheng and H. Y. Xu, *J. Phys. Chem. C*, 2014, **118**, 7010–7017.
35 S. K. Ko, Y. K. Yang, J. Tase and I. Shin, *J. Am. Chem. Soc.*, 2006, **128**, 14150–14155.
36 Y. K. Yang, K. J. Yook and J. Tae, *J. Am. Chem. Soc.*, 2005, **127**, 16760–16761.
37 J. Y. Kwon, Y. J. Jang, Y. J. Lee, K. M. Kim, M. S. Seo, W. Nam and J. Yoon, *J. Am. Chem. Soc.*, 2005, **127**, 10107–10111.
38 V. Dujols, F. Ford and A. W. Czarnik, *J. Am. Chem. Soc.*, 1997, **119**, 7386–7387.
39 Y. L. Leng, J. H. Zhang, Q. Li, Y. M. Zhang, Q. Lin, H. Yao and T. B. Wei, *Spectrochim. Acta, Part A*, 2016, **167**, 116–121.
40 W. J. Qu, W. T. Li, H. L. Zhang, T. B. Wei, Q. Lin, H. Yao and Y. M. Zhang, *Spectrochim. Acta, Part B*, 2017, **241**, 430–437.
41 B. B. Shi, P. Zhang, T. B. Wei, H. Yao, Q. Lin and Y. M. Zhang, *Chem. Commun.*, 2013, **49**, 7812–7814.

